JOURNAL OF PROPULSION AND POWER
Vol. 25, No. 3, May–June 2009

Performance Evaluation of a Fast Mobility-Based Particle Spectrometer for Aircraft Exhaust

Donald E. Hagen,* Prem Lobo,† Philip D. Whitefield,‡ Max B. Trueblood,§ and Darryl J. Alofs¶
Missouri University of Science and Technology, Rolla, Missouri 65409
and
Otmar Schmid**
Helmholtz Zentrum München, D-85758 Neuherberg/Munich, Germany

DOI: 10.2514/1.37654

The Cambustion DMS500, a novel aerosol sizing instrument with fast time resolution, was first employed to sample jet engine particulate matter emissions during Project APEX. This paper compares the performance of the DMS500 to that of traditional aerosol instruments for sampling jet engine exhaust aerosol under field conditions during this campaign. The observed geometric mean diameter with respect to the particle number (D_g) ranged from 15 to 45 nm, and with respect to the mass (third moment) distribution (D_{gM}) from 21 to 112 nm, the geometric standard deviation (σ_g) ranged from 1.22 to 1.90 and the total number concentration (N) ranged from 6×10^3 to $3.3 \times 10^5/\text{cm}^3$ (after dilution). On average, the D_g, D_{gM}, σ_g, and N of the DMS500 size distributions differed by −9, −7, +1, and +30% from the reference values of the traditional instruments. Compared with the reference values, both D_g and σ_g of the DMS500 showed a small but statistically significant decrease with increasing particle size. Effects due to particle shape appeared to be the most likely explanation for the observed size-related trends. The 30% disagreement in concentration measurements is reasonable when the sensitivity of the 3022 condensation particle counter to pressure fluctuations encountered during measurements at the engine exhaust nozzle is taken into account.

Nomenclature

D_g	=	number-based geometric mean diameter
D_{gM}	=	mass-based geometric mean diameter
D_p	=	particle diameter
N	=	total number concentration
P	=	penetration coefficient
σ_g	=	geometric standard deviation

I. Introduction

IN RECENT years the particulate matter size distributions from jet engines have been characterized using standard aerosol methodologies employing differential mobility analysis [1–3]. This technique is limited because it does not have the approximately 1 Hz time resolution to allow synchronization with the combustion gas measurements acquired using current recommended practices prescribed by the International Civil Aviation Organization under Annex 16, Volume 2 of the Chicago Convention. This paper compares the performance of a novel aerosol sizing instrument with fast time resolution (DMS500) to that of traditional aerosol instruments for measuring jet engine exhaust aerosol.

A. Background

The application of electrical mobility (particle migration in an electric field) to determine the size of airborne ions and charged particles extends back to the beginning of the 20th century [4]. Commercial instruments became available in the 1960s, but these instruments were only suited for aerosol with slowly varying size distribution. More recently, advancements such as the scanning differential mobility analyzer (SDMA), a prime example being the TSI SMPS [5], have reduced the sampling time for measuring a complete particle size distribution between approximately 5 and 800 nm to below 2 min. Although SDMA systems have become the most widely used sizing technique for submicron aerosol particles [6–11], numerous applications require sampling rates of about 1 Hz, such as process control of nanoparticle synthesis or optimization of non-steady-state (transient) combustion processes.

Recently, Tammet et al. [12] introduced a different type of mobility spectrometer called the electrical aerosol spectrometer (EAS) with a time resolution on the order of seconds. Variants of the EAS like the Cambustion DMS500 [13] and the TSI engine exhaust particle sizer (EEPS) [14] have recently become commercially available. In contrast to the SDMA, which sequentially monitors different particle size bins using a single particle detector downstream of a classification column with gradually changing electric field, the DMS500 simultaneously characterizes selected size bins with a cascade of electrometers connected to a classification column with time-invariant electric field. Although both the SDMA and DMS500 operate on the same principle of electrical mobility, there are numerous technical differences related to all of the main components, namely aerosol charging, classification column, and particle detection, which makes it necessary to compare the performance of the SDMA and DMS500 for different types of challenge aerosols.

Because commercial versions of the DMS500 have only become available within the past few years [13], there is very limited information available on their performance for different types of aerosols. Recently, DMS500 systems have been applied to tobacco

Received 20 March 2008; revision received 7 January 2009; accepted for publication 31 January 2009.

*Professor of Physics and Director of the Cloud and Aerosol Sciences Laboratory, Center of Excellence for Aerospace Particulate Emissions Reduction Research, G-7 Norwood Hall; hagen@mst.edu.

†Assistant Director, Center of Excellence for Aerospace Particulate Emissions Reduction Research, G-7 Norwood Hall; plobo@mst.edu. Member AIAA.

‡Professor and Chair of Chemistry and Director of Center of Excellence for Aerospace Particulate Emissions Reduction Research, G-7 Norwood Hall; pwhite@mst.edu. Member AIAA.

§Senior Research Aide, Center of Excellence for Aerospace Particulate Emissions Reduction Research, G-7 Norwood Hall; trueblud@mst.edu.

¶Professor of Mechanical Engineering, Center of Excellence for Aerospace Particulate Emissions Reduction Research, G-7 Norwood Hall; dalofs@mst.edu.

**Senior Scientist, Institute of Inhalation Biology, Ingolstädter Landstrasse 1; otmar.schmid@helmholtz-muenchen.de; also Adjunct Assistant Professor, Missouri University of Science and Technology.

smoke [15], laser ablation fugitive emissions [16], and diesel emissions [17–19].

There is a substantial SDMA database on particulate size distributions from various aircraft engines [2,20–23]. The use of fast sizing instruments such as the DMS500 would be advantageous, because engine on-time for sampling is expensive, some engine conditions (e.g., takeoff power) can be made available only for short times, and it would allow observations of engine transients between stable operating conditions. However, in the arena of gas turbine emissions measurement, the instruments have to perform in environments having significantly more electronic noise, acoustic noise, and fluctuations in sample line pressure than in normal laboratory settings. There was concern that due to technical differences between the traditional instruments [SDMA and condensation particle counter (CPC)] and fast spectrometers and the results of some preliminary intercomparison measurements, that the fast electrometer based spectrometers (EEPS and DMS500) may not be applicable to this harsh environment and/or the measured size distributions would be inconsistent with the large body of engine emission data mainly obtained from SDMA and CPC systems. However, the potential value of fast spectrometer analysis to jet engine testing warrants further in-depth analysis to validate or refute these concerns.

Hence, in this study we compare the performance of a conventional SDMA and CPC with a novel DMS500 for submicron particles from a gas turbine engine acquired during a field campaign. We briefly discuss the major differences between these instruments, present the experimental setup, and compare the sizing and counting performance of the DMS500 with that of an SDMA and a CPC, respectively, under the harsh operating conditions in the vicinity of a gas turbine engine.

B. Differences Between SDMA and DMS500

In this study we employed a Cambustion DMS500 (Cambustion, Ltd., Cambridge, UK), a TSI SDMA consisting of a differential mobility analyzer [differential mobility analyzer (DMA), model 3071, TSI, Shoreview, MN] and a CPC (model 3025, TSI). In addition, we determined total particle number concentration using a TSI 3022 CPC. The performances of the TSI SDMA and CPC have been investigated thoroughly in the literature [6,24–29].

Although both the DMS500 and the SDMA operate on the principle of electrical mobility, there are significant differences in all major components. Table 1 lists the technical details of the DMS500 and SDMA and the operating conditions chosen for this intercomparison study. After passing through an aerodynamic separator (cyclone or impactor) and an electrostatic charger, the particles enter a classification column followed by a particle detection system. Although the particles are transported axially through the annular classification column, which consists of a central rod held at high voltage and a grounded, coaxial outer rod, the charged particles follow a specific trajectory depending on their electrical mobility and, hence, on their charge-to-diameter ratio (equivalent mobility diameter). Significant differences exist between the DMS500 and the SDMA for the aerosol charger, classification columns, particle detection, and data inversion.

The DMS500 and the SDMA use fundamentally different charging techniques. The former generates unipolarly charged particles (positive) with a corona diffusion charger, and the latter employs radioactive diffusion charging to generate both negatively and positively charged particles, where only the negatively charged fraction is used for size classification. Precise knowledge of the established charge distribution is essential for retrieval of the particle size distribution from the raw data in both devices using different inversion routines. Among other parameters the bipolar charge distribution depends not only on particle size but on particle shape and the composition of the carrier gas [30]. Unipolar charging is even more sensitive to the latter two parameters, and it introduces a number of additional complications such as elevated loss of charged particles in the charger and potential generation of artifact sulfuric acid particles in the high electric field near the corona discharge, if sufficient amounts of SO_2 and H_2O are present in the carrier gas (particularly relevant for sampling combustion exhaust) [30–32]. In addition, unlike the bipolar charger, already positively charged aerosol cannot be neutralized by the unipolar charger, because only positively charged ions are generated. Consequently, the charge distribution exiting the corona charger depends on the (positive) charging state of the challenge aerosol. Because this most likely affects particles smaller than 50 nm, where the charging efficiency of the unipolar charger is lowest, charged particles below 50 nm are electrostatically removed upstream of the charger by an electrostatic precipitator. The main differences regarding the classification columns of the two instruments are that the electric field is spatially invariant but varied with time in the SDMA, whereas in the DMS500 the electric field is time-invariant but increasing with axial location. Furthermore, the DMS500 uses 26 electrometers connected to metal rings at the outer rim of the classification column for particle detection, whereas the SDMA draws all particles within a narrow mobility range through a slit in the central rod for subsequent detection with a CPC. Consequently, the inversion routine [31] of the DMS500, converting the raw electrometer signals into particle number size distribution, is significantly more complicated than that of the SDMA [8] mainly due to the larger number of charge states occurring for unipolar charging and the fact that each electrometer ring has a different transfer function. Finally, for nonspherical particles, such as those typically encountered during combustion

Table 1 Technical details and operating conditions for the TSI SDMA (DMA 3071, CPC 3022) and Cambustion DMS500

Technical aspect	SDMA	DMS500
Aerodynamic separator (cut-off diameter)	Impactor, 1000 nm	Cylone, 1000 nm
Electrostatic precipitator	---	Removal of charged particles, <50 nm
Electrical charger type	Radioactive diffusion charger, Po^{210}	Corona diffusion charger
Charging state	Bipolar (negative used for sizing)	Uniploar (positive)
Classification column		
Sample/sheath flow rate, liter/min	1.4/9.0	8.0/30
Pressure, hPa	~1000, ambient	250
Geometry of classification column		
Length, mm	444.4	700
Outer diameter, mm	19.58	53
Inner diameter, mm	9.37	25
Voltage		
Maximum value, kV	10	7
Temporal variability	Yes	No
Axial variability	No	Yes
Minimum sampling time, s	35 (here 100)	<1 (here ~7)
Size range, nm	~10–700 (here 10–340)	3–1000
Particle detection	1 CPC	26 Electrometers

exhaust measurements, particle alignment effects may systematically bias particle sizing in both devices [33].

In summary, although both instruments operate on the same sizing principle (electrical mobility), there are substantial technical differences, which require consistency tests of the DMS500 and SDMA.

II. Experimental Setup, Quality Assurance, and Data Analysis

The first parallel measurements of aircraft exhaust particulates with a conventional SDMA and a DMS500 were conducted during Project APEX (aircraft particle emissions experiment). This study was a multi-agency collaborative research effort, performed at the NASA Dryden Flight Research Center at Edwards Air Force Base in California during April 2004. The goals of the project were to characterize aircraft emissions, their evolution in the near-field of the engine exit plane, and the demonstration of the viability of new characterization technologies. In particular, parametric studies were performed at different engine operating conditions to characterize particle and trace gas precursor species in the emissions from a NASA DC-8 aircraft with CFM56-2C1 engines at selected locations (1 m, 10 m, and 30 m) downstream of the engine exit plane [23]. A detailed description of the results obtained at APEX using the DMS500 is reported by Lobo et al. [34].

Only data from the 1 m sampling probe were used for this intercomparison analysis, because the data from the 10 m and 30 m probes exhibited lower signal-to-noise ratios and more time variation due to crosswind interference. Two series of runs were performed during Project APEX: one using NASA-selected run criteria and one using EPA- (Environmental Protection Agency) selected criteria. Both were included in this analysis. The EPA cycles followed the landing takeoff (LTO) cycle with the following sequence of power conditions and sampling durations: 7% (17 min), 100% (0.7 min), 85% (2.2 min), 30% (4 min), 7% (17 min). The NASA sampling sequence generally followed the following power (duration) scheme: 4% (4 min), 100% (1.5 min), 85% (4 min), 70% (4 min), 65% (4 min), 40% (4 min), 30% (4 min), 15% (4 min), 7% (4 min), 4% (4 min). However, some data were also taken at power settings of 5.5%, 60%, and pre-ground idle. For each power setting, data were taken with the DMS500, SDMA, and CPC, and these data, encompassing 300 runs, are intercompared in this study.

Continuous sampling was performed in a standard configuration [1], which had been used on previous measurement campaigns characterizing jet engine emissions [35–41]. In brief, a dilution flow of clean, dry gas (nitrogen) was normally added to the sample at the probe tip in order to suppress particle interactions and condensation. The dilution was substantial, varied from run to run, and reduced concentrations by a factor of between about 10 and 100, with an average and standard deviation of 41 and 22, respectively. The extracted sample was distributed through the NASA Langley Research Center (LaRC) distribution system to several research groups (Fig. 1), including the Missouri University of Science and Technology (Missouri S&T), previously known as University of Missouri–Rolla.

Particle loss in the transport lines was experimentally determined for each segment of the sampling train. For the intercomparison study the crucial line losses were those between the subject instruments (DMS500, SDMA, and CPC) and the distribution plenum in the Missouri S&T mobile laboratory, because the line loss between the Missouri S&T distribution plenum and the probe was common to all the instruments. The particle line losses were experimentally determined with monodisperse sodium chloride particles, and mathematically described by polynomial fits in $\ln D_p$, where D_p represents the (equivalent mobility) diameter. Figure 2 shows the experimentally determined penetration coefficient P between the three instruments and the distribution plenum. Although these penetration curves can be implemented directly into the inversion routines of the DMS500 and SDMA, the correction factor for the CPC (P(CPC)) depends on the individual run's size distribution and is determined as the number weighted mean of the penetration curve.

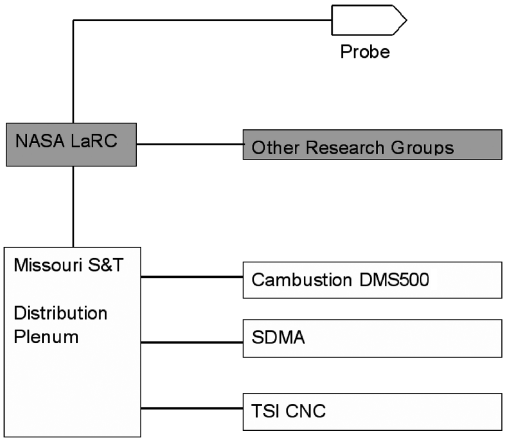

Fig. 1 Schematic of instrumental setup.

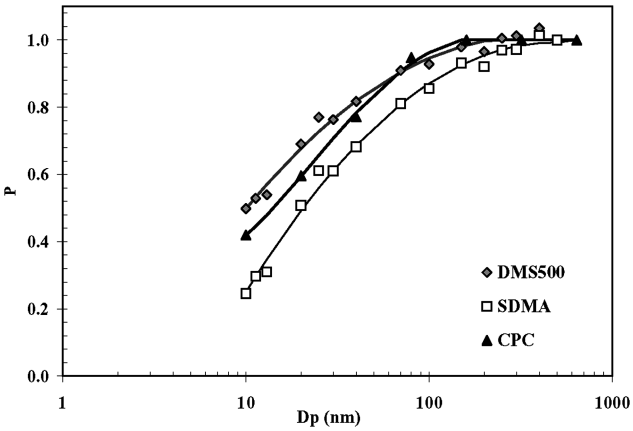

Fig. 2 Experimentally determined penetration coefficients through the transport lines to the DMS500, SDMA, and CPC.

During this intercomparison experiment typical size-averaged P(CPC) values were around 0.70 ± 0.05.

Theoretically, the DMS500 may be operated at a sampling rate of up to 10 Hz. However, the sampling frequency for a complete size distribution may be significantly reduced by 1) signal smearing effects due to nonuniform velocity profiles in the transport lines and 2) the need to collect a statistically meaningful sample, that is, sufficient concentration in each size bin. In the APEX study, the time needed for obtaining a DMS500 size distribution between 5 and 1000 nm was typically 7 s (compared with 100 s for the SDMA size distribution between 10 and 340 nm). The operating conditions of the SDMA and the DMS500 are listed in Table 1. During any given engine setting, typically 2 and 20 size distributions were obtained with the SDMA and DMS500, respectively. The smaller size range of the SDMA has no significant impact on the intercomparison results, because the SDMA detected at least 95% of the number and mass distribution for all data points presented here.

An additional complication was introduced by the fact that the DMS500 operates at 250 hPa, whereas the SDMA and the CPC operate at line pressure. For constant line pressure, the DMS500 software automatically takes pressure into account. However, for variable operating pressure as encountered here due to the varying engine power (inlet pressure) and varying sample dilution, two additional correction factors had to be applied to the DMS500. Periodically (a few times during a measurement day) the DMS500 was put through a calibration procedure called autozeroing, which sets the nominal line pressure for the run and determines the noise level of the electrometers. This was done with the engine operating at idle, which puts the probe close to ambient pressure. The DMS500 uses a mass flow meter to determine the flow rate through its front-end critical orifice. The mass flow rate of gas through the orifice will vary in proportion to the ratio of sample line pressure during a

measurement to that during the autozero, and the instrument's aerosol differential concentrations must be corrected by the reciprocal of this ratio. Also, the aerosol bin diameters (particle diameters corresponding to bin index) will change with pressure. Pressures higher than that at autozero will cause higher linear velocities through the measurement region, particles will travel farther before impacting an electrometer, and hence will be perceived as having a larger diameter. A manufacturer-supplied formula giving correct bin diameters as a function of pressure is available for pressure variations up to ±40%. An interpolation procedure was performed after the bin diameter correction in order to determine the aerosol size spectrum at a consistent set of particle diameters. The actual sample line pressure was provided to the DMS500 via an analog input channel and was imbedded into the DMS500's normal data stream, simplifying subsequent data reduction activity.

During Project APEX engine power varied between 4 and 100%. The corresponding sample line pressure variation with respect to the DMS500s autozero pressure was from −3 to +36%, values within the range for which the DMS500s pressure corrections are applicable. The mass flow rate correction to the differential concentrations was thus in the range +3 to −36%, and the bin size corrections were in the range from +0.6 to −9%, respectively.

All instrument flow rates and main operating parameters were calibrated on-site. In addition, the sizing accuracy of the SDMA and DMS500 was confirmed with spherical particles of known size (polystyrene latex spheres with a nominal diameter of 50–1000 nm), and the DMS500 was calibrated for smaller sizes with DMA-selected nucleated liquid sulfuric acid (less than 15 nm), atomized and dried sulfuric acid (15–30 nm), and atomized and dried solid salt particles (20–60 nm).

During Project APEX, 154 emission sampling runs were performed using the 1 m probe. As a measure of quality assurance, we screened the data for source stability and effects due to background aerosol. Source stability was judged based on both SDMA and DMS500 data. If the percentage difference in the SDMA geometric mean diameters of two consecutive size scans exceeded 20%, the data was excluded for the intercomparison. Similarly, if the standard deviation of the DMS500 geometric mean diameters (typically 20 values per engine setting) exceeded 20% of its average, the run was not used. Periodically, the concentration of the atmospheric background aerosol was measured. If the particle concentration signal to background ratio was less than 4 (due to, for example, significant cross winds), the run was excluded, because the intercomparison was to be for aircraft-generated not atmospheric aerosols. Using these criteria, 102 of the 154 runs passed the selection criteria and were included in the analysis.

III. Results and Discussion

To quantify differences in instrument performance, four characteristic parameters were considered: number-based geometric mean diameter (D_g), geometric standard deviation (σ_g), mass-based (third moment) geometric mean diameter (D_{gM}), and total number concentration (N), where D_g and D_{gM} are more representative for the smaller- and large-size fraction for a given size distribution, respectively. For the Project APEX data set of 300 runs used for the intercomparison, the observed D_g values ranged from 15 to 45 nm, D_{gM} from 21 to 112 nm, σ_g from 1.22 to 1.90, and N from 6×10^3 to $3.3 \times 10^5/\text{cm}^3$ (at the instruments after a 10 to 100 fold dilution). Sample size distribution plots from the DMS500 and the SDMA are shown in Fig. 3 for an engine idle run, which was the most common power condition sampled in the campaign.

A linear regression analysis of D_g and σ_g for the DMS500 (ordinate) and SDMA (abscissa) is given in Fig. 4. A scatter plot comparison of this data shows significant deviation from ideality with a slope, intercept, and correlation coefficient (R^2) of 0.69 (1.24), 5.5 nm (−0.37), and 0.67 (0.61), respectively. On the other hand, the campaign average of the D_g, D_{gM}, and σ_g ratios of DMS500 to SDMA are 0.91, 0.93, and 1.01 with a variability of 16, 26, and 6.5% about the mean, respectively, and the average particle number concentration of the DMS500 is 30% larger than that of the CPC

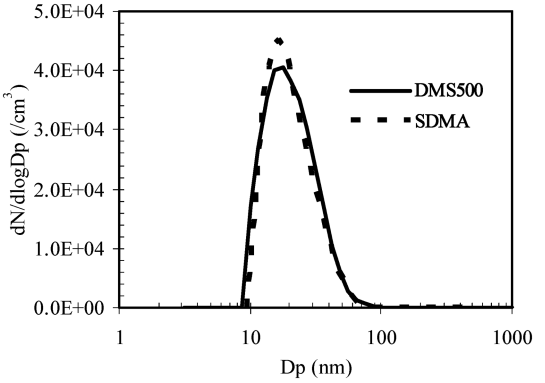

Fig. 3 Size distributions for engine idle exhaust using baseline fuel.

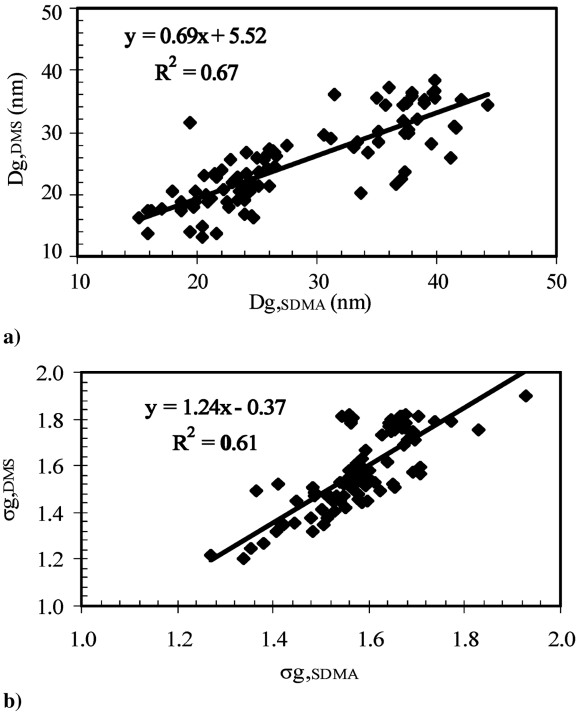

Fig. 4 Scatter plot of a) geometric mean diameters, and b) geometric standard deviations of the particle size distributions measured by the SDMA and DMS500.

(Table 2). Hence, in spite of considerable scatter in the APEX data, which is at least partially due to unavoidable instabilities in the challenge aerosol and the harsh experimental conditions, the average D_g, D_{gM}, σ_g, and N of the DMS500 agree to within 9, 7, 1, and 30%, respectively, with the corresponding reference values. Laboratory experiments conducted after the APEX campaign to compare the DMS500 and the CPC showed somewhat better DMS500-CPC agreement in N (14%). A more recent laboratory intercomparison between the DMS500 and a TSI CPC (3022) and SDMA (3071) was conducted using NaCl aerosols with mean sizes 19, 39, 48, 87, 119, and 122 nm in diameter. For all instruments (DMS500, SDMA, and CPC) the repeatability in all the characteristic parameters for multiple measurements of the size distribution for a constant aerosol was 1% or better. The average difference between the DMS500 and the SDMA was 5% for geometric mean diameter and 4% for total concentration, and between the DMS500 and the CPC it was 18% for total concentration. An intercomparison experiment conducted at NASA Langley in 1999 reported [42] variations between CPCs in the range from 10 to 20%. An estimated uncertainty [1] for laboratory-condition work is 3.3% for DMA-based size measurement and 18% for CPC-based total concentration measurement. Hence, during laboratory tests, differences between the DMS500 and the reference

Table 2 Summary of the DMS500, SDMA, and CPC comparison for geometric mean diameter, geometric standard deviation, mass-based (3rd moment) geometric mean diameter, and number concentration

Parameter	Mean	Variability
$D_{g,\mathrm{DMS}}/D_{g,\mathrm{SDMA}}$	0.91	16%
$\sigma_{g,\mathrm{DMS}}/\sigma_{g,\mathrm{SDMA}}$	1.01	6.5%
$D_{gM,\mathrm{DMS}}/D_{gM,\mathrm{SDMA}}$	0.93	26%
$N_{\mathrm{DMS}}/N_{\mathrm{CPC}}$	1.30	33%

instruments are comparable to the uncertainties in the DMA and CPC reported elsewhere [1,42]. In the project APEX campaign the differences are larger. For geometric mean the difference goes up by a factor 1.8, from 5 to 9%; for total concentration it goes up by a factor 1.7, from 18 to 30%.

Some of the difference in total concentration may be due to the response of the TSI 3022 CPC to pressure fluctuations. The CPC is affected more strongly by pressure fluctuations than is the DMS500. The 3022 computes a total concentration based on an anticipated volumetric flow rate of the sample through the counting volume rather than a measured flow rate. This flow rate is influenced by sample pressure. The sample line pressure during an engine test point measurement period does fluctuate by up to 5%. The standard deviation of the CPCs concentration measurement during test points is consistently greater than that of the DMS500 by a factor of more than 3.

Insight into the potential reasons for the observed deviations between the DMS500 and SDMA can be obtained from Fig. 5, which shows that the D_g and σ_g ratios of the DMS500 to SDMA decrease systematically from about 1.05 to 0.8 and 1.06 to 0.96, respectively, as D_g increases from about 15 to 45 nm, where clearly the former is significantly more pronounced than the latter. Considering the technical differences between the DMS500 and the SDMA listed in Table 1, one possible reason for the observed trends could be the removal of charged particles smaller than 50 nm upstream of the DMS500 corona charger in order to avoid artifacts in the charge distribution as described previously. Although this effect was minimized during Project APEX by passing the sample aerosol through a neutralizer (bipolar charger; not shown in Fig. 1), it is instructive to assess the expected bias in $D_{g,\mathrm{DMS}}$ and $\sigma_{g,\mathrm{DMS}}$. If we assume that the particles entering the corona charger had reached charge equilibrium and that all particles less than 50 nm diameter were removed upstream of the corona charger, we can estimate the effect of particle removal by replacing the removed particles back into the DMS500 particle distribution using the charge distribution by Wiedensohler [43]. As seen from Fig. 6, this correction results in a -2 to $+2$% change in $D_{g,\mathrm{DMS}}$ depending on particle size. If almost the entire size distribution is below 50 nm, the mean size shifts to larger values because the faction of charged particles increases with particle size. On the other hand, for size distributions centered around 50 nm, $D_{g,\mathrm{DMS}}$ shifts to smaller sizes because only charged particles smaller than 50 nm are removed, that is, the correction enhances the small but not the large end of the size distribution. A similar rationale explains the observed small trend in $\sigma_{g,\mathrm{DMS}}$ (Fig. 6b). It is evident from Fig. 6 that accounting for the removal of charged particles would enhance the trends in D_g and σ_g ratio (Fig. 5) resulting in slopes of -0.0084 and -0.0046, respectively, and somewhat better linear correlation coefficients (R^2) of 0.19 and 0.27, respectively. This suggests that the removal of particles smaller than 50 nm from the DMS500 did not play a significant role during APEX. Another explanation for the observed trends in the D_g and σ_g ratios could be elevated diffusional losses in the DMS500 (or the SDMA). However, because smaller particles are more affected by diffusion than larger

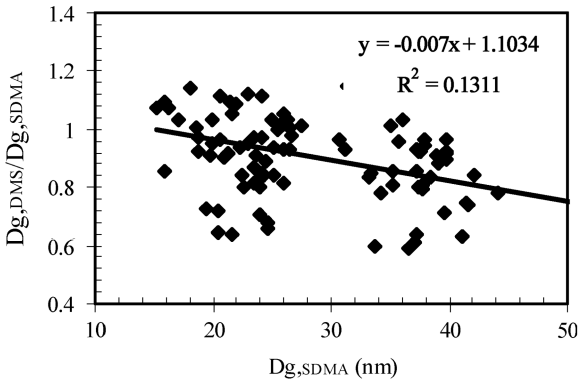

a)

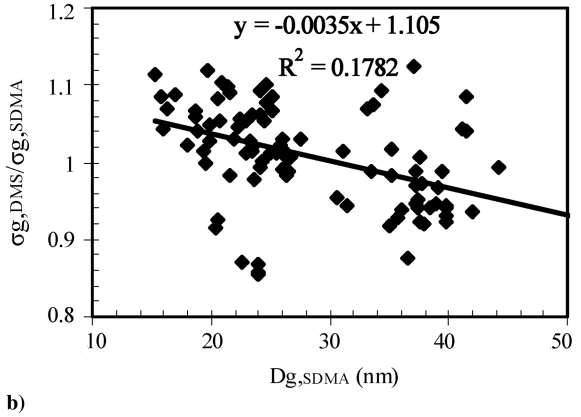

b)

Fig. 5 Ratio of DMS500 to SDMA a) geometric mean diameter, and b) geometric standard deviations as a function of SDMA geometric mean diameter.

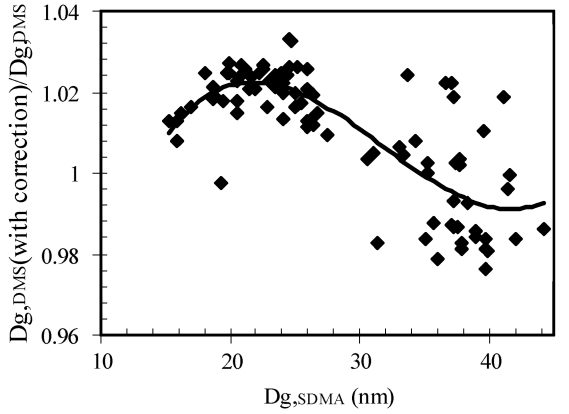

a)

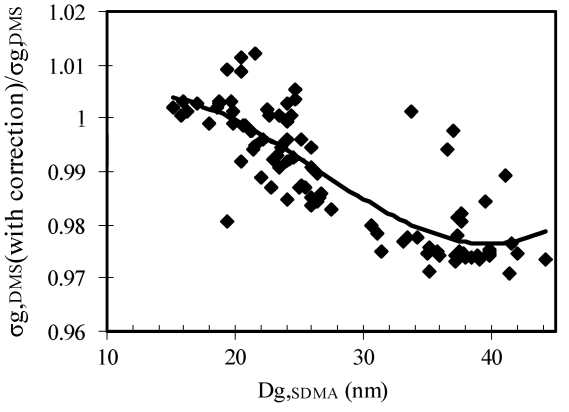

b)

Fig. 6 The effect of the removal of charged particles smaller than 50 nm upstream of the DMS500 corona charger on the a) measured geometric mean diameter, and b) geometric standard deviation as a function of SDMA geometric mean diameter.

ones, diffusion cannot account for the observed large differences (approximately 20%) between $D_{g,\mathrm{DMS}}$ and $D_{g,\mathrm{SDMA}}$ at the large end of the size spectrum. As mentioned previously, the high electric field near the corona discharge of the DMS500 may generate artifact sulfuric acid particles in nucleation mode (diameter less than 15 nm), if sufficient amounts of SO_2 and H_2O are present in the carrier gas. However, no evidence was found for this artifact during Project APEX because the DMS500 size spectra did not contain elevated levels of nucleation-mode particles (diameter less than 15 nm) for more than 90% of the data. Another possible explanation for the observed trend in the D_g and σ_g ratios could be the nonspherical shape of aircraft emission particles. Finally, it is conceivable that due to the large variation in line pressure between 572 and 896 hPa during APEX, a bias in the manufacturer-provided pressure correction for the DMS500 may have contributed to the observed trend in D_g ratio (Fig. 5a). However, because there is no correlation between line pressure and D_g ($R^2 = 0.0002$), the observed weak systematic decrease in D_g ratio with increasing pressure (from 0.95 to 0.85) will only contribute to the observed scatter but not to the systematic trend in D_g ratio. Analogous to our results, Symonds et al. [19] have recently shown that, for nonspherical diesel soot agglomerates, the D_g ratio of DMS500 to SDMA decreases with increasing particle size. They observed D_g ratios near unity for almost-spherical particles (small agglomerates consisting of only a few spherical primary particles) and D_g ratios as low as 0.65 for larger, more nonspherical particles. This trend was attributed to the sensitivity of the DMS500 charge distribution on particle shape. It is of interest to note that an analogous sensitivity would be expected for the SDMA. Although diesel soot is found to be more agglomerated than aircraft soot exhaust, larger aircraft exhaust particles are more likely to be nonspherical (agglomerated) than smaller ones [1], and this could at least partially explain the negative trend in the D_g ratio for aircraft particulates as shown in Fig. 5a.

In summary, considering the harsh experimental conditions in the vicinity of a gas turbine engine and the fact that the size and concentration measurement techniques (DMS500 vs SDMA and CPC) differ significantly, there is reasonable agreement between the DMS500 and the reference instruments (SDMA and CPC) for engine exhaust particulate matter measurements.

In the case of sizing data, the disagreement between instruments is less than 10%. No evidence was found for inadvertent generation of sulfuric acid (or other nucleation mode) particles from gaseous precursors in the high electric field of the DMS500 charging unit. Although small effects due to 1) the removal of charged particles smaller than 50 nm upstream of the DMS500 corona charger, 2) unaccounted diffusional losses in the DMS500 and/or the SDMA, and 3) the sensitivity of the charging units on trace gas composition can not be ruled out, the observed decrease in $D_{g,\mathrm{DMS}}$ (and $D_{gM,\mathrm{DMS}}$; data not shown) with increasing particle size is consistent with observations for diesel soot particles [19], which were attributed to the sensitivity of the DMS500 charger to particle shape.

In the case of concentration measurements, the disagreement is 30%, which is greater than that found for well-controlled laboratory experiments. However, this is a reasonable result when the sensitivity of the 3022 CPC to pressure fluctuations encountered during measurements at the engine exhaust nozzle is taken into account.

IV. Conclusions

The wealth of particle data taken during project APEX with DMS500, SDMA, and CPC instruments provided a unique opportunity to intercompare the performance of these instruments under the harsh sampling conditions near a gas turbine aircraft engine. In spite of considerable scatter in the data set, which is at least partially due to unavoidable instabilities in the challenge aerosol and the harsh experimental conditions, the average D_g, D_{gM}, σ_g, and N of the DMS500 agree to within -9, -7, $+1$, and $+30\%$, respectively, with the corresponding reference values derived from SDMA and CPC data. The negative systematic DMS500 trends in D_g and to a much lesser degree in σ_g with increasing particles size is likely due to the sensitivity of the DMS500 charging efficiency to particle shape. No evidence for significant artifacts due to other adverse effects was found. Considering the differences in the measurement techniques and the harsh experimental conditions, this represents satisfactory agreement between the DMS500 and the reference instruments (SDMA and CPC). However, our study also suggests that the consistency of the DMS500 and SDMA data needs to be verified, if (partially) nonspherical particles in carrier gases with varying (trace gas) composition are investigated, which is particularly relevant for the sampling of combustion-derived particles. Therefore, in conclusion, the generally satisfactory agreement between the DMS500 and the SDMA and the much shorter sampling time of the DMS500, suggests using a DMS500 instead of a SDMA will significantly reduce the cost for engine emission tests due to reduced engine sampling times.

Acknowledgments

The authors would like to acknowledge the sponsorship of NASA (Chowen Wey, project manager), through cooperative agreement NCC3-1084, and the Missouri University of Science and Technology Center of Excellence for Aerospace Particulate Emissions Reduction Research throughout the work described in this paper.

References

[1] Schmid, O., Hagen, D. E., Whitefield, P. D., Trueblood, M. B., Rutter, A. P., and Lilenfeld, H. V., "Methodology for Particle Characterization in the Exhaust Flows of Gas Turbine Engines," *Aerosol Science and Technology*, Vol. 38, No. 11, 2004, pp. 1108–1122. doi:10.1080/027868290507222

[2] Paladino, J. D., Hagen, D. E., Whitefield, P. D., Hopkins, A. R., Schmid, O., Wilson, M. R., Schlager, H., and Schulte, P., "Observations of Particulates Within the North Atlantic Flight Corridor: POLINAT 2, September–October 1997," *Journal of Geophysical Research*, Vol. 105, No. D3, 2000, pp. 3719–3726. doi:10.1029/1999JD901071

[3] Schumann, U., Schlager, H., Arnold, F., Ovarlez, J., Kelder, H., Hov, O., Hayman, G., Issaksen, I. S. A., Staehelin, J., and Whitefield, P. D., "Pollution from Aircraft Emissions in the North Atlantic Flight Corridor: Overview on the POLINAT Projects," *Journal of Geophysical Research*, Vol. 105, No. D3, 2000, pp. 3605–3631. doi:10.1029/1999JD900941

[4] Flagan, R. C., "History of Electrical Aerosol Measurements," *Aerosol Science and Technology*, Vol. 28, No. 4, 1998, pp. 301–380. doi:10.1080/02786829808965530

[5] Wang, S. C., and Flagan, R. C., "Scanning Electrical Mobility Spectrometer," *Aerosol Science and Technology*, Vol. 13, No. 2, 1990, pp. 230–240. doi:10.1080/02786829008959441

[6] Knutson, E. O., and Whitby, K. T., "Accurate Measurements of Aerosol Electric Mobility Moments," *Journal of Aerosol Science*, Vol. 6, No. 6, 1975, pp. 453–460.

[7] Kousaka, Y., Okuyama, K., and Endo, Y., "Calibration of Differential Mobility Analyzer by Visual Method," *Journal of Aerosol Science*, Vol. 12, No. 4, 1981, pp. 339–348. doi:10.1016/0021-8502(81)90023-9

[8] Hagen, D. E., and Alofs, D. J., "A Linear Inversion Method to Obtain Aerosol Size Distributions from Measurements with a Differential Mobility Analyzer," *Aerosol Science and Technology*, Vol. 2, No. 4, 1983, pp. 465–475. doi:10.1080/02786828308958650

[9] Stolzenburg, M. R., "An Ultrafine Aerosol Size Measuring System," Ph.D. Dissertation, University of Minnesota, Minneapolis, MN, 1998.

[10] Reischl, G. P., "Measurement of Ambient Aerosols by the Differential Mobility Analyzer Method: Concepts and Realization Criteria for the Size Range Between 2 and 500 nm," *Aerosol Science and Technology*, Vol. 14, No. 1, 1991, pp. 5–24. doi:10.1080/02786829108959467

[11] Zhang, S. H., Akutsu, Y., Russell, L. M., Flagan, R. C., and Seinfeld, J. H., "Radial Differential Mobility Analyzer," *Aerosol Science and Technology*, Vol. 23, No. 3, 1995, pp. 357–372. doi:10.1080/02786829508965320

[12] Tammet, H., Mirme, A., and Tamm, E., "Electrical Aerosol Spectrometer of Tartu University," *Atmospheric Research*, Vol. 62, Nos. 3–4, 2002, pp. 315–324. doi:10.1016/S0169-8095(02)00017-0

[13] Reavell, K., Hands, T., and Collings, N., "A Fast Response Particulate Spectrometer for Combustion Aerosols," Society of Automotive Engineers Technical Paper 2002-01-2714, Warrendale, PA, 2002.

[14] Johnson, T., Caldow, R., Pöscher, A., Mirme, A., and Kittelson, D., "New Electrical Mobility Particle Sizer Spectrometer for Engine Exhaust Particle Measurements," Society of Automotive Engineers Technical Paper 2004-01-1341, Warrendale, PA, 2004.

[15] McAughey, J., and McGrath, C., "Ageing of Sidestream and Environmental Tobacco Smoke," *Proceedings of the 24th Annual AAAR Conference*, American Association for Aerosol Research, Paper 1PB6, Mt. Laurel, NJ, 2005.

[16] Gensdarmes, F., and Vendel, J., "Real Time Measurement of Fugitive Nanoparticle Emission," *Proceedings of the 24th Annual AAAR Conference*, American Association for Aerosol Research, Paper 1PC11, Mt. Laurel, NJ, 2005.

[17] Biskos, G., Reavell, K., Hands, T., and Collins, N., "Fast Measurements of Aerosol Spectra," *Journal of Aerosol Science*, Vol. 34, No. S1, 2003, pp. S67–S68.

[18] Hands, T., and Nickolaus, C., "Real Time Diesel Particulate Filter Efficiency Measurements from Spectral Data," *Proceedings of the 24th Annual AAAR Conference*, American Association for Aerosol Research, Paper 8PH15, Mt. Laurel, NJ, 2005.

[19] Symonds, J. P. R., Reavell, K., Olfert, J. S., Campbell, B. W., and Swift, S. J., "Diesel Soot Mass Calculation in Real-Time with a Differential Mobility Spectrometer," *Journal of Aerosol Science*, Vol. 38, No. 1, 2007, pp. 52–68.
doi:10.1016/j.jaerosci.2006.10.001

[20] Hagen, D. E., Paladino, J., Whitefield, P. D., Trueblood, M. B., and Lilenfeld, H. V., "Airborne and Ground Based Jet Engine Aerosol Emissions Sampling During Two NASA Field Projects: SUCCESS and SNIF," *Journal of Aerosol Science*, Vol. 28, No. S1, 1997, pp. S67–S68.
doi:10.1016/S0021-8502(97)85034-3

[21] Petzold, A., Fiebig, M., Fritzsche, L., Stein, C., Schumann, U., Wilson, C. W., Hurley, C. D., Arnold, F., Katragkou, E., Baltensperger, U., Gysel, M., Nyeki, S., Hitzenberger, R., Giebl, H., Hughes, K. J., Kurtenbach, R., Wiesen, P., Madden, P., Puxbaum, H., Vrchoticky, S., and Wahl, C., "Particle Emissions from Aircraft Engines—A Survey of the European Project PartEmis," *Meterologische Zeitschrift*, Vol. 14, No. 4, 2005, pp. 465–476.
doi:10.1127/0941-2948/2005/0054

[22] Anderson, B. E., Branham, H. S., Hudgins, C. H., Plant, J. V., Ballenthin, J. O., Miller, T. M., Viggiano, A. A., Blake, D. R., Boudries, H., Canagaratna, M., Maike–Lye, R. C., Onasch, T., Wormhoudt, J., Worsnop, D., Brunke, K. E., Culler, S., Penko, P., Sanders, T., Han, H.-S., Lee, P., Pui, D. Y. H., Thornhill, K. L., and Winstead, E. L., "Experiment to Characterize Aircraft Volatile Aerosol and Trace-Species Emissions (EXCAVATE)," NASA TM-2005-213783, Hampton, VA, Aug. 2005.

[23] Wey, C. C., Anderson, B. A., Wey, C., Miake–Lye, R. C., Whitefield, P., and Howard, R., "Overview on the Aircraft Particle Emissions eXperiment (APEX)," *Journal of Propulsion and Power*, Vol. 23, No. 5, 2007, pp. 898–905.
doi:10.2514/1.26406

[24] Hewitt, G. W., "The Charging of Small Particles for Electrostatic Precipitation," *Transactions of the American Institute of Electrical Engineers*, Vol. 76, 1957, pp. 300–306.

[25] Whitby, K. T., and Clark, W. E., "Electric Aerosol Particle Counting and Size Distribution Measuring System for the 0.015 to 1 μ Size Range," *Tellus*, Vol. 18, 1966, pp. 573–586.

[26] Liu, B. Y. H., and Pui, D. Y. H., "A Submicron Aerosol Standard and the Primary Absolute Calibration of the Condensation Nucleus Counter," *Journal of Colloid Interface Science*, Vol. 47, No. 1, 1974, pp. 155–171.
doi:10.1016/0021-9797(74)90090-3

[27] Knutson, E. O., and Whitby, K. T., "Aerosol Classification by Electric Mobility: Apparatus, Theory, and Applications," *Journal of Aerosol Science*, Vol. 6, No. 6, 1975, pp. 443–451.
doi:10.1016/0021-8502(75)90060-9

[28] Agarwal, J. K., and Sem, G., "Continuous Flow, Single-Particle-Counting Condensation Nucleus Counter," *Journal of Aerosol Science*, Vol. 11, No. 4, 1980, pp. 343–357.
doi:10.1016/0021-8502(80)90042-7

[29] Quant, F. R., Caldow, R., Sem, G. J., and Addison, T. J., "Performance of Condensation Particle Counters with Three Continuous-Flow Designs," *Journal of Aerosol Science*, Vol. 23, No. S1, 1992, pp. 405–408.
doi:10.1016/0021-8502(92)90435-X

[30] Biskos, G., Mastorakos, E., and Collings, N., "Monte-Carlo Simulation of Unipolar Diffusion Charging for Spherical and Non-Spherical Particles," *Journal of Aerosol Science*, Vol. 35, No. 6, 2004, pp. 707–735.
doi:10.1016/j.jaerosci.2003.11.010

[31] Biskos, G., Reavell, K., and Collings, N., "Description and Theoretical Analysis of a Differential Mobility Spectrometer," *Aerosol Science and Technology*, Vol. 39, No. 6, 2005, pp. 527–541.
doi:10.1080/027868291004832

[32] Biskos, G., Reavell, K., and Collings, N., "Unipolar Diffusion Charging of Aerosol Particles in the Transition Regime," *Journal of Aerosol Science*, Vol. 36, No. 2, 2005, pp. 247–265.
doi:10.1016/j.jaerosci.2004.09.002

[33] Zelenyuk, A., Cai, Y., and Imre, D., "From Agglomerates of Spheres to Irregularly Shaped Particles: Determination of Dynamic Shape Factors from Measurements of Mobility and Vacuum Aerodynamic Diameters," *Aerosol Science and Technology*, Vol. 40, No. 3, 2006, pp. 197–217.
doi:10.1080/02786820500529406

[34] Lobo, P., Hagen, D. E., Whitefield, P. D., and Alofs, D. J., "Physical Characterization of Aerosol Emissions from a Commercial Gas Turbine Engine," *Journal of Propulsion and Power*, Vol. 23, No. 5, 2007, pp. 919–929.
doi:10.2514/1.26772

[35] Hagen, D. E., Trueblood, M. B., and Whitefield, P. D., "A Field Sampling of Jet Exhaust Aerosols," *Particulate Science and Technology*, Vol. 10, Nos. 1–2, 1992, pp. 53–63.
doi:10.1080/02726359208906598

[36] Hagen, D. E., and Whitefield, P. D., "Particulate Emissions in the Exhaust Plume from Commercial Jet Aircraft Under Cruise Conditions," *Journal of Geophysical Research Atmospheres*, Vol. 101, No. D14, 1996, pp. 19551–19557.
doi:10.1029/95JD03276

[37] Hagen, D., Whitefield, P., Paladino, J., Trueblood, M., and Lilenfeld, H., "Particulate Sizing and Emission Indices for a Jet Engine Exhaust Sampled at Cruise," *Geophysical Research Letters*, Vol. 25, No. 10, 1998, pp. 1681–1684.
doi:10.1029/97GL03504

[38] Hagen, D. E., Whitefield, P. D., Paladino, J., Schmid, O., Schlager, H., and Schulte, S. P., "Atmospheric Aerosol Measurements in the North Atlantic Flight Corridor During Project POLINAT-2," *Journal of Aerosol Science*, Vol. 30, No. S1, 1999, pp. S161–S162.
doi:10.1016/S0021-8502(99)80092-5

[39] Hagen, D. E., and Whitefield, P. D., "A Study of the Fate of Carbonaceous Aerosol Emissions Through a Gas Turbine Engine," *Proceedings of the A&WMA Annual Conference and Exhibition*, Air & Waste Management Association, Pittsburg, PA, 2003.

[40] Petzold, A., Busen, R., Baumann, R., Kuhn, M., Strom, J., Hagen, D., Whitefield, P., Baumgardner, D., Arnold, F., Borrmann, S., and Schumann, U., "Near Field Measurements on Contrail Properties from Fuels with Different Sulfur Content," *Journal of Geophysical Research*, Vol. 102, No. D25, 1997, pp. 29867–29880.
doi:10.1029/97JD02209

[41] Whitefield, P. D., Ross, M., Hagen, D. E., and Hopkins, A., "Aerosol Characterization in Rocket Plumes," *Journal of Aerosol Science*, Vol. 30, No. S1, 1999, pp. S215–S216.
doi:10.1016/S0021-8502(99)80119-0

[42] Cofer, W. R., Jr., Anderson, B. E., Connors, V. S., Wey, C. C., Sanders, T., Twohy, C., Brock, C. A., Winstead, E. L., Pui, D., Chen, D., Hagen, D. E., and Whitefield, P. "NASA's Atmospheric Effects of Aviation Project: Results of the August 1999 Aerosol Measurement Intercomparison Workshop, Laboratory Phase," NASA TM-2001-210829, National Technical Information Service, Springfield, VA, June 2001.

[43] Wiedensohler, A., "An Approximation of the Bipolar Charge Distribution for Particles in the Submicron Range," *Journal of Aerosol Science*, Vol. 19, No. 3, 1988, pp. 387–389.
doi:10.1016/0021-8502(88)90278-9

L. Maurice
Associate Editor